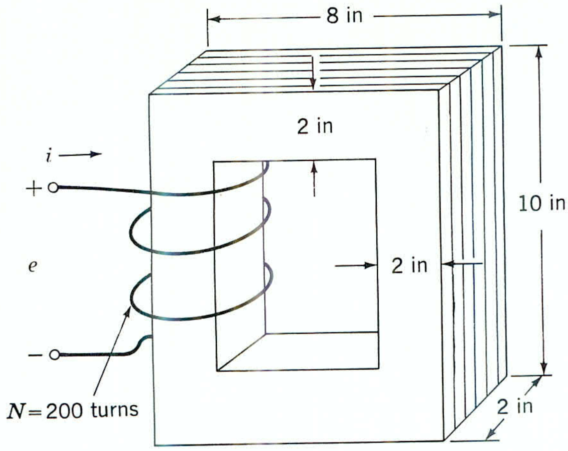

Fig. 1-14. Reactor with laminated steel core.

1-5 PERMANENT MAGNETS

Figure 1-15*a* shows the second quadrant of a hysteresis loop for Alnico 5, a typical permanent magnet material, while Fig. 1-15*b* shows the second quadrant of a hysteresis loop for M-5 steel.† Notice that the curves are similar in nature. However, the hysteresis loop of Alnico 5 is characterized by a large value of *residual flux density* or *remanent magnetization* B_r (approximately 1.22 Wb/m^2) as well as a large value of *coercivity* H_c (approximately −49 kA/m). The remanent magnetization B_r corresponds to the flux density which would remain in a closed magnetic structure, such as that of Fig. 1-1, made of this material if the applied mmf (and hence the magnetic field intensity H) were reduced to zero. However, although the M-5 electrical steel also has a large value of remanent magnetization (approximately 1.4 Wb/m^2), it has a much smaller value of coercivity (approximately −6 A/m, smaller by a factor of over 7500).

The significance of remanent magnetization is that it can result in the presence of magnetic flux in a magnetic circuit in the absence of external excitation in the form of currents in windings. This is a well-known phenomenon. It is commonplace in applications ranging from magnets which hold notes on refrigerator doors to small permanent magnet appliance motors and loudspeakers.

From Fig. 1-15, it would appear that both Alnico 5 and the M-5 electrical steel would be useful in producing flux in unexcited magnetic circuits since they both have large values of remanent magnetization. That this is not the case can be best illustrated by an example.

†To obtain the largest value of remanent magnetization, the hysteresis loops of Fig. 1-15 are those which would be obtained if the materials were excited by sufficient mmf to ensure that they were driven heavily into saturation. This is discussed further in Art. 1-6.

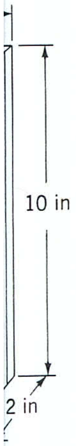

ıs loop for Alnico 5, a
5b shows the second
that the curves are
ico 5 is characterized
nagnetization B_r (ap-
percivity H_c (approxi-
B_r corresponds to the
ic structure, such as
mmf (and hence the
owever, although the
nent magnetization
value of coercivity
500).
at it can result in the
e absence of external
is a well-known phe-
from magnets which
nagnet appliance mo-

5 and the M-5 electri-
ted magnetic circuits
tization. That this is

ysteresis loops of Fig. 1-15
ed by sufficient mmf to en-
cussed further in Art. 1-6.

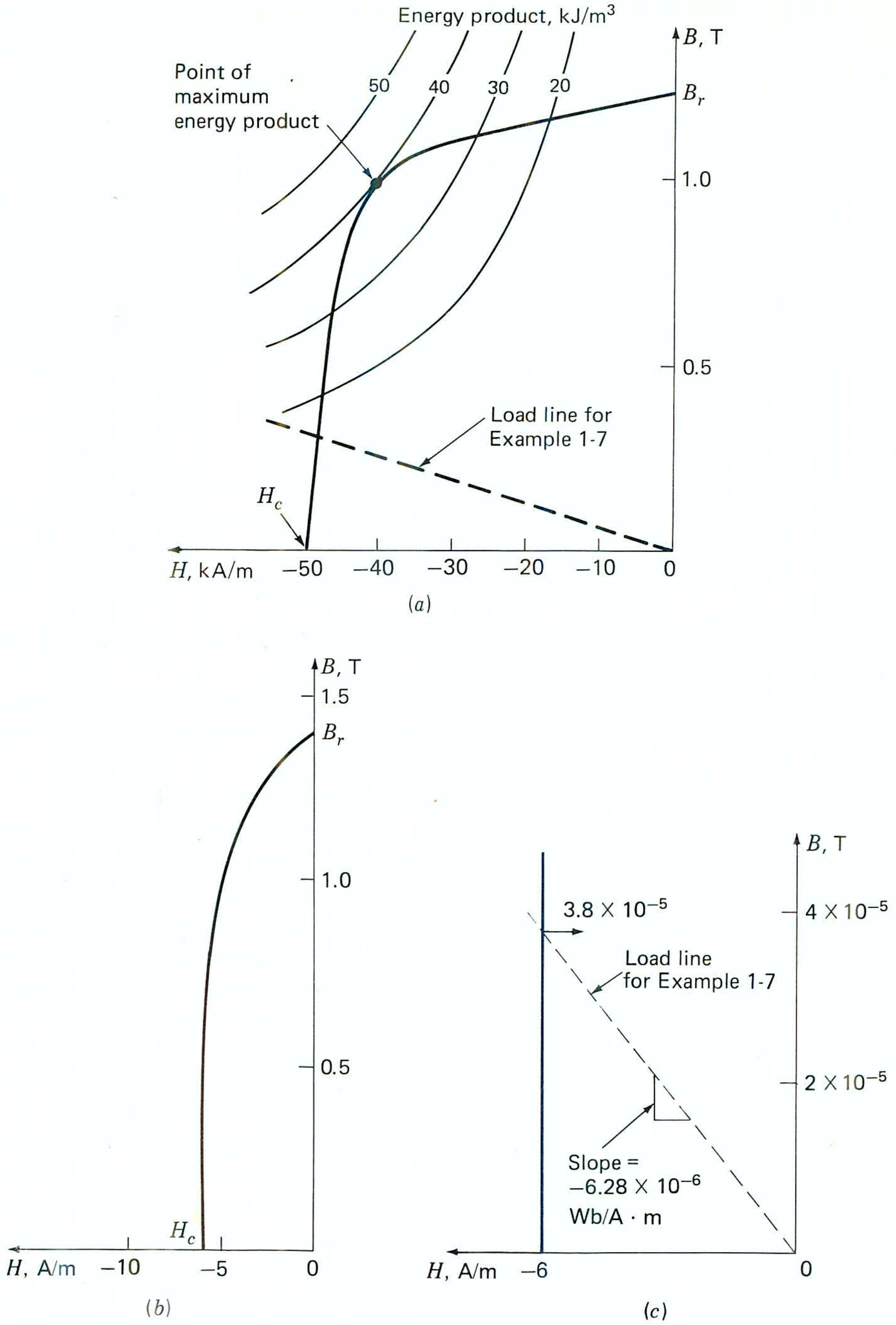

Fig. 1-15. (*a*) Second quadrant of hysteresis loop for Alnico 5; (*b*) second quadrant of hysteresis loop for M-5 electrical steel; (*c*) hysteresis loop for M-5 electrical steel expanded for small *B*. (*Armco Inc.*)

EXAMPLE 1-7

As shown in Fig. 1-16, a magnetic circuit consists of a core of high permeability ($\mu \rightarrow \infty$), an air gap of length g, and a section of magnetic material of length l_m. Calculate the flux density B_g in the air gap if the magnetic material is (*a*) Alnico 5 and (*b*) M-5 electrical steel.

Solution

(*a*) Since the core permeability is assumed infinite, we neglect H in the core as negligible. Recognizing that the mmf acting on the magnetic circuit of Fig. 1-16 is zero, we can write

$$\mathcal{F} = 0 = H_g g + H_m l_m$$

or

$$H_g = -\frac{l_m}{g} H_m$$

where H_g and H_m are the magnetic field intensities in the air gap and the magnetic material, respectively.

Since the flux must be continuous through the magnetic circuit,

$$\phi = A_g B_g = A_m B_m$$

or

$$B_g = \frac{A_m}{A_g} B_m$$

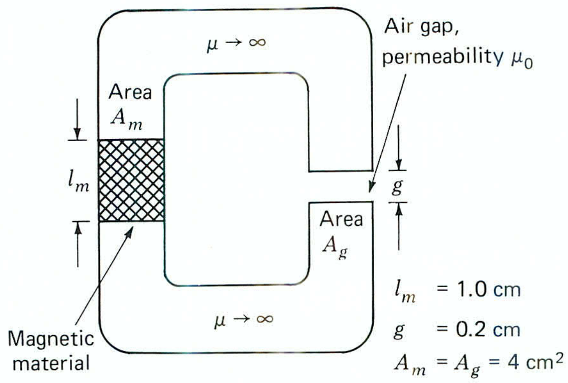

Fig. 1-16. Magnetic circuit for Example 1-7.

where B_g and B_m are the magnetic flux densities in the air gap and the magnetic material, respectively.

These equations can be solved to yield a linear relationship for B_m in terms of H_m:

$$B_m = -\mu_0 \left(\frac{A_g}{A_m}\right)\left(\frac{l_m}{g}\right) H_m = -5\mu_0 H_m = -6.28 \times 10^{-6} H_m$$

To solve for B_m, we recognize that Alnico 5, B_m, and H_m are also related by the curve of Fig. 1-15*a*. Thus this linear relationship, also known as the *load line*, can be plotted on Fig. 1-15*a* and the solution obtained graphically, resulting in

$$B_g = B_m = 0.30 \text{ T}$$

(*b*) The solution for M-5 electrical steel proceeds exactly as in part (*a*). The load line is the same as that of part (*a*) because it is determined only by the permeability of the air gap and the geometries of the magnet and the air gap. Hence from Fig. 1-15*c*

$$B_g = 3.8 \times 10^{-5} \text{ T} = 0.38 \text{ G}$$

which is much less than the value obtained with Alnico 5.

Example 1-7 shows that there is an immense difference between permanent magnet materials (often referred to as hard magnetic materials) such as Alnico 5 and soft magnetic materials such as M-5 electrical steel. This difference is characterized in large part by the immense difference in their coercivities H_c. The coercivity can be thought of as a measure of the amount of mmf required to demagnetize the material. As seen from Example 1-7, it is also a measure of the capability of the material to produce flux in a magnetic circuit which includes an air gap. Thus we see that materials which make good permanent magnets are characterized by large values of coercivity H_c (considerably in excess of 1 kA/m).

A useful measure of the capability of a permanent magnet is known as its *maximum energy product*. This corresponds to the largest B-H product $(BH)_{max}$, which corresponds to a point on the second quadrant of the hysteresis loop. As we have seen, the product of B and H has the dimensions of energy density (joules per cubic meter). We now show that operation of a given permanent magnet material at this point will result in the smallest volume of that material required to produce a given flux density in the air gap. Similarly, choosing a material with the largest available maximum energy product will result in the smallest required magnet volume.

In Example 1-7, we found an expression for the flux density in the air gap:

$$B_g = \frac{A_m}{A_g} B_m \tag{1-49}$$

We also found that the ratio of the mmf drops across the magnet and the air gap is equal to −1:

$$\frac{H_m l_m}{H_g g} = -1 \tag{1-50}$$

Equation 1-50 can be solved for $B_g = \mu_0 Hg$, and the result can be multiplied by Eq. 1-49 to yield

$$\begin{aligned} B_g^2 &= \mu_0 \left(\frac{l_m A_m}{g A_g} \right) (-H_m B_m) \\ &= \mu_0 \left(\frac{\text{vol}_{\text{mag}}}{\text{vol}_{\text{air gap}}} \right) (-H_m B_m) \end{aligned} \tag{1-51}$$

or

$$\text{vol}_{\text{mag}} = \frac{B_g^2 \text{vol}_{\text{air gap}}}{\mu_0 (-H_m B_m)} \tag{1-52}$$

where vol_{mag} is the volume of the magnet, $\text{vol}_{\text{air gap}}$ is the air-gap volume, and the minus sign arises because, at the operating point of the magnetic circuit, H in the magnet (H_m) is negative.

Equation 1-52 is the desired result. It indicates that to achieve a desired flux density in the air gap, the required volume of the magnet can be minimized by operating the magnet at the point of the maximum B-H product, i.e., the *point of maximum energy product*. Because the maximum energy product is a measure of the magnet volume required for a given application, it is often found as a tabulated "figure of merit" on data sheets for permanent magnet materials.

Note that Eq. 1-51 appears to indicate that one can achieve an arbitrarily large air-gap flux density simply by reducing the air-gap volume. This is not true in practice because as the flux density in the magnetic circuit increases, a point will be reached at which the magnetic core material will begin to saturate and the assumption of infinite permeability will no longer be valid, thus invalidating Eq. 1-51.

Note that a curve of constant B-H product is a hyperbola. A set of such hyperbolas for different values of the B-H product is plotted in Fig. 1-15*a*. From these curves, we see that the maximum energy product for Alnico 5 is 40 kJ/m^3 and that this occurs at the point $B = 1.0$ Wb/m^2 and $H = -40$ kA/m.

(1-49)

e magnet and the

(1-50)

ult can be multi-

(1-51)

(1-52)

air-gap volume,
of the magnetic

to achieve a de-
e magnet can be
maximum B-H
se the maximum
d for a given ap-
" on data sheets

achieve an arbi-
air-gap volume.
he magnetic cir-
ic core material
eability will no

la. A set of such
d in Fig. 1-15a.
uct for Alnico 5
b/m^2 and H =

EXAMPLE 1-8

The magnetic circuit of Fig. 1-16 is modified so that the air-gap area is reduced to $A_g = 2.0\ \text{cm}^2$ as shown in Fig. 1-17. Find the minimum magnet volume required to achieve an air-gap flux density of 0.8 T.

Solution

The smallest magnet volume will be achieved with the magnet operating at its point of maximum energy product, as shown in Fig. 1-15a. At this operating point, $B_m = 1.0$ T and $H_m = -40$ kA/m.

Thus from Eq. 1-49,

$$\begin{aligned} A_m &= A_g \frac{B_g}{B_m} \\ &= (2\ \text{cm}^2)\left(\frac{0.8}{1.0}\right) = 1.6\ \text{cm}^2 \end{aligned}$$

and from Eq. 1-50,

$$\begin{aligned} l_m &= -g\frac{H_g}{H_m} = -g\frac{B_g}{\mu_0 H_m} \\ &= -0.2\ \text{cm}\frac{0.8}{(4\pi \times 10^{-7})(-40 \times 10^3)} \\ &= 3.18\ \text{cm} \end{aligned}$$

Thus the minimum magnet volume is equal to $1.6 \times 3.18 = 5.09\ \text{cm}^3$.

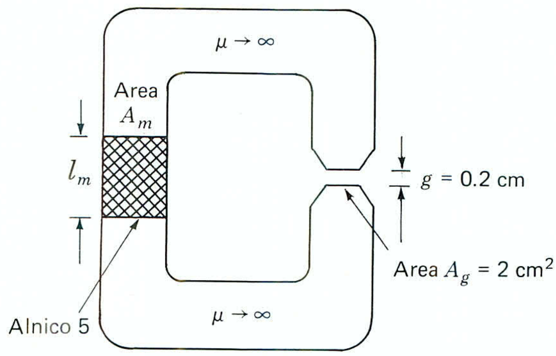

Fig. 1-17. Magnetic circuit for Example 1-8.

1-6 APPLICATION OF PERMANENT MAGNET MATERIALS

Examples 1-7 and 1-8 consider the operation of hard magnetic materials under the assumption that the operating point can be determined simply from a knowledge of the geometry of the magnetic circuit and the properties of the various magnetic materials involved. In fact, the situation is more complex.† This section will expand upon these issues.

Figure 1-18 shows the dc magnetization characteristics for a few common permanent magnet materials. Alnico 5 is a widely used version of an alloy of iron, nickel, aluminum, and cobalt originally discovered in 1931. It has a relatively large residual flux density. Alnico 8 has a lower residual flux density and a higher coercivity than Alnico 5. It is hence less subject to demagnetization than Alnico 5. Disadvantages of the Alnico materials are their relatively low coercivity and their mechanical brittleness.

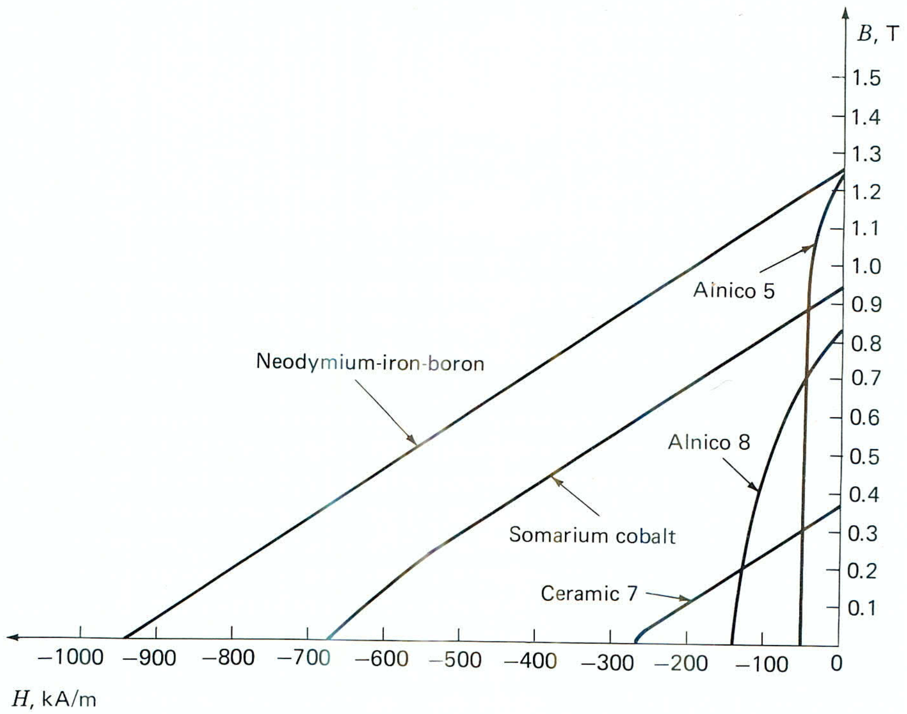

Fig. 1-18. DC magnetization curves for common permanent magnet materials.

†For a further discussion of permanent magnets and their applications, see F. N. Bradley, *Materials for Magnetic Functions,* Hayden Book Co., New York, 1971, chap. 4; G. R. Slemon and A. Straughen, *Electric Machines,* Addison-Wesley, Reading, Mass., 1980, secs. 1.20–1.25; and C. Heck, *Magnetic Materials and Their Applications,* Butterworth & Co., London, 1974, chap. 9.

Ceramic permanent magnet materials (also known as *ferrite magnets*) are made from iron oxide and barium or strontium carbonate powders and have lower residual flux densities than Alnico materials but significantly higher coercivities. As a result, they are much less prone to demagnetization. One such material, ceramic 7, is shown in Fig. 1-18, where its dc magnetization characteristic is almost a straight line. Ceramic magnets have good mechanical characteristics and are inexpensive to manufacture; as a result, they are the most widely used of permanent magnet materials.

Somarium cobalt represents a significant advance in permanent magnet technology which began in the 1960s with the discovery of rare-earth permanent magnet materials. From Fig. 1-18 it can be seen to have a high residual flux density such as is found with the Alnico materials, while at the same time having a much higher coercivity and maximum energy product.

The newest of the rare-earth magnetic materials is the neodymium-iron-boron material. It features even larger residual flux density, coercivity, and maximum energy product than does somarium cobalt. In addition, it has good mechanical properties and is relatively inexpensive to manufacture and thus can be expected to find increasing use in permanent magnet applications.

Consider the magnetic circuit of Fig. 1-19. This consists of a section of hard magnetic material in a core of highly permeable soft magnetic material. An N-turn excitation winding is also included. With reference to Fig. 1-20, we assume that the hard magnetic material is initially unmagnetized and consider what happens as current is applied to the excitation winding. Because the core is assumed to be of infinite permeability, the horizontal axis of Fig. 1-20 can be considered to be both a measure of the applied current $i = Hl_m/N$ as well as a measure of H in the magnetic material.

As current i is increased to its maximum value, the B-H trajectory rises from point a in Fig. 1-20 toward its maximum value at point b. To fully magnetize the material, we assume that the current has been in-

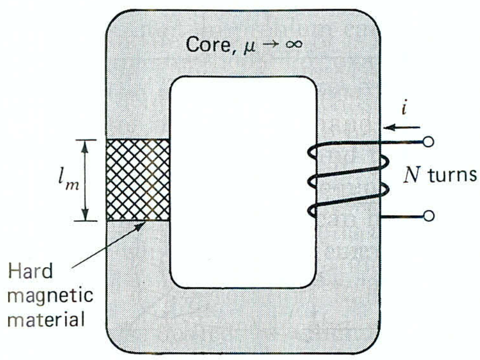

Fig. 1-19. Magnetic circuit including both a permanent magnet and an excitation winding.

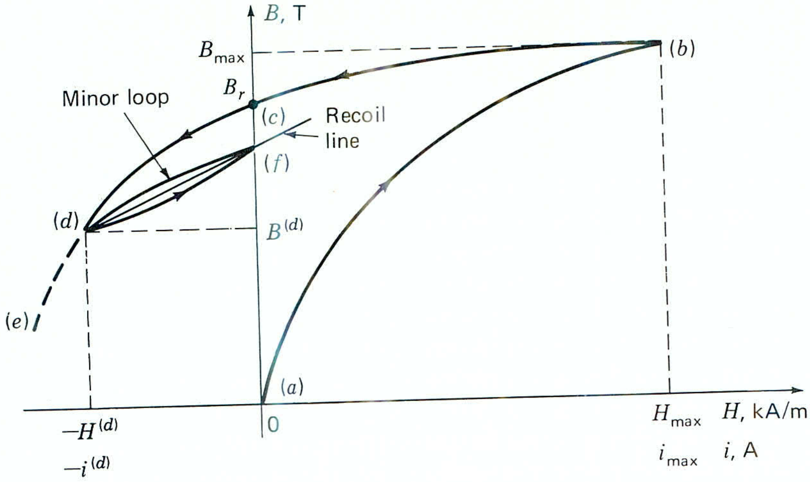

Fig. 1-20. Portion of a *B-H* characteristic showing a minor loop and a recoil line.

creased to a value i_{max} sufficiently large that the material has been driven well into saturation at point *b*. When the current is then decreased to zero, the *B-H* characteristic will begin to form a hysteresis loop, arriving at point *c* at zero current. At point *c*, notice that *H* in the material is zero but *B* is at its remanent value B_r.

As the current then goes negative, the *B-H* characteristic continues to trace out a hysteresis loop. In Fig. 1-20, this is seen as the trajectory between points *c* and *d*. If the current is then maintained at the value $-i^{(d)}$, the operating point of the magnet will be that of point *d*. Note that, as in Example 1-7, this same operating point would be reached if the material were to start at point *c* and, with the excitation held at zero, an air gap of length $g = l_m(A_g/A_m)(-\mu_0 H^{(d)}/B^{(d)})$ were then inserted in the core.

Should the current then be made more negative, the trajectory would continue tracing out the hysteresis loop toward point *e*. However, if instead the current is reduced to zero, the trajectory does not in general retrace the hysteresis loop toward point *c*. Rather it begins to trace out a *minor hysteresis loop,* reaching point *f* when the current reaches zero. If the current is then varied between zero and $-i^{(d)}$, the *B-H* characteristic will trace out the minor loop as shown.

As can be seen from Fig. 1-20, the *B-H* trajectory between points *d* and *f* can be represented by a straight line, known as the *recoil line*. The slope of this line is called the *recoil permeability* μ_R. We see that once this material has been demagnetized to point *d*, the effective remanent magnetization of the magnetic material is that of point *f* which is less than the remanent magnetization B_r which would be expected based on the hysteresis loop. Note that should the demagnetization be increased past point *d*, for example, to point *e* of Fig. 1-20, a new minor loop will be created, with a new recoil line and recoil permeability.

The demagnetization effects of negative excitation which have just been discussed are equivalent to those of an air gap in the magnetic circuit. For example, clearly the magnetic circuit of Fig. 1-19 could be used as a device to magnetize hard magnetic materials. The process would simply require that a large excitation be applied to the winding and then reduced to zero, leaving the material at a remanent magnetization B_r (point c in Fig. 1-20).

Following this magnetization process, if the material were removed from the core, this would be equivalent to opening a large air gap in the magnetic circuit, demagnetizing the material in a fashion similar to that seen in Example 1-7. At this point, the magnet has been effectively weakened, since if it were again inserted in the magnetic core, it would follow a recoil line and return to a remanent magnetization somewhat less than B_r. Thus hard magnetic materials often do not operate stably in situations with varying mmf and geometry, and there is often the risk that improper operation can further demagnetize them.

At the expense of a reduction in value of the remanent magnetization, hard magnetic materials can be stabilized to operate over a specified region. This procedure, based on the recoil trajectory shown in Fig. 1-20, can best be illustrated by an example.

EXAMPLE 1-9

Figure 1-21 shows a magnetic circuit containing hard magnetic material, a core and plunger of high (assumed infinite) permeability, and a single-turn winding which will be used to magnetize the hard magnetic material. The winding will be removed after the system is magnetized. The plunger

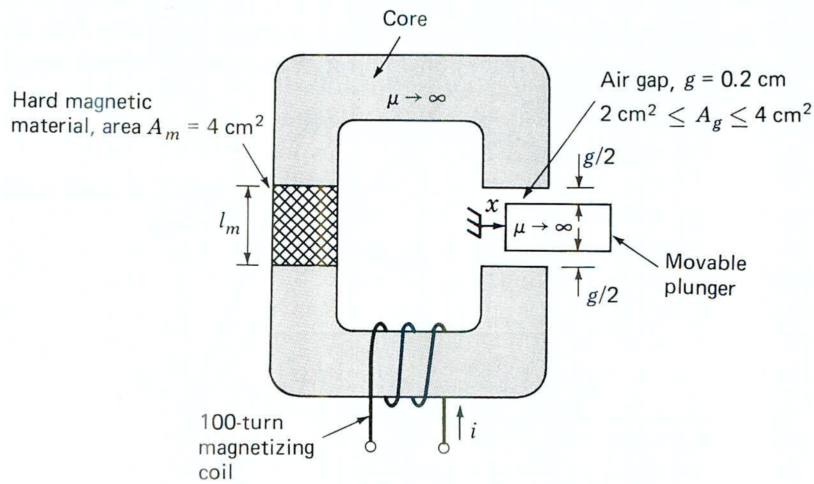

Fig. 1-21. Magnetic circuit for Example 1-9.

moves in the x direction as indicated, with the result that the air-gap area can vary ($2\ \text{cm}^2 \le A_g \le 4\ \text{cm}^2$). Assuming that the hard magnetic material is Alnico 5, (a) find the magnet length l_m so that the system will operate on a recoil line which intersects the maximum B-H product point on the magnetization curve for Alnico 5, (b) derive a procedure for magnetizing the magnet, and (c) calculate the flux density B_g in the air gap as the plunger moves.

Solution

(a) Figure 1-22a shows the magnetization curve for Alnico 5 and two load lines corresponding to the two extremes of the air gap, $A_g = 2\ \text{cm}^2$ and $A_g = 4\ \text{cm}^2$. We see that the system will operate on the desired recoil line if the load line for $A_g = 2\ \text{cm}^2$ intersects the B-H characteristic at the maximum energy product point (labeled point a in Fig. 1-22a), $B_m^{(a)} = 1.0$ T and $H_m^{(a)} = -40$ kA/m.

From Eqs. 1-49 and 1-50, we see that the slope of the required load line is given by

$$\frac{B_m^{(a)}}{-H_m^{(a)}} = \frac{B_g}{H_g}\frac{A_g}{A_m}\frac{l_m}{g}$$

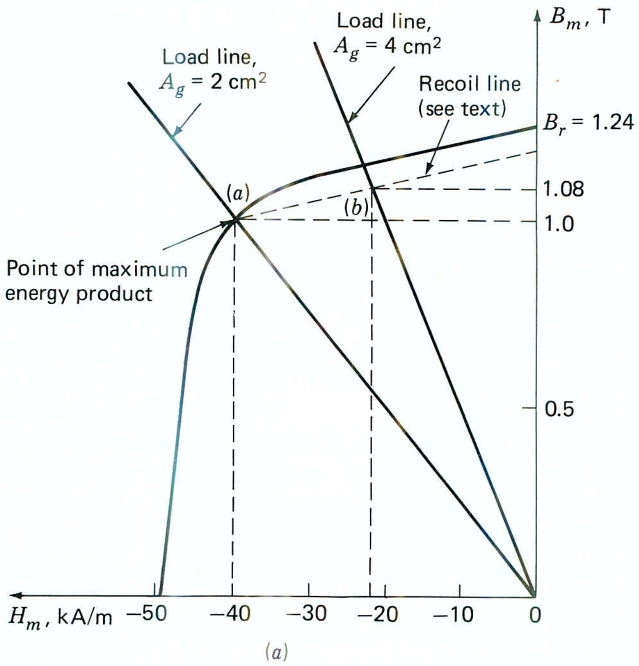

Fig. 1-22. (a) Magnetization curve for Alnico 5 for Example 1-9; (b) series of load lines for $A_g = 2\ \text{cm}^2$ and varying values of i showing the magnetization procedure for Example 1-9.

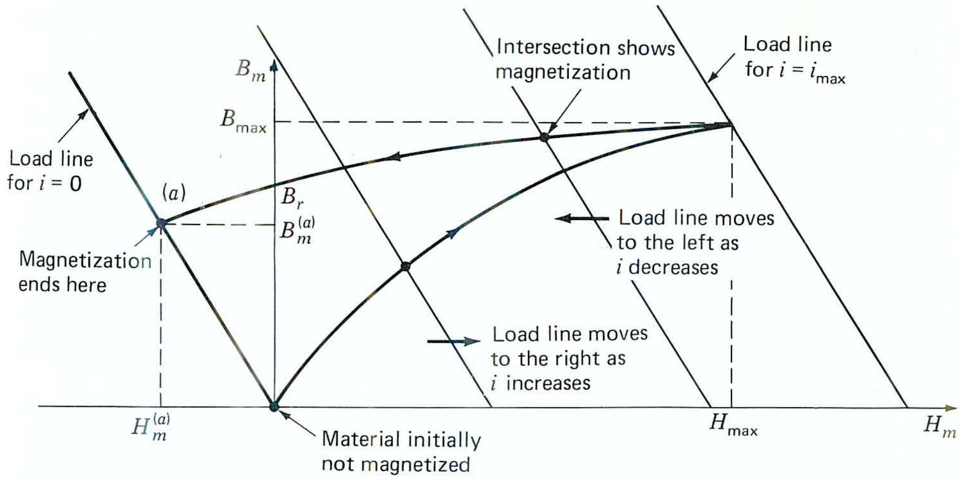

(b)

Fig. 1-22. *(Continued).*

and thus

$$l_m = g\left(\frac{A_m}{A_g}\right)\left(\frac{B_m^{(a)}}{-\mu_0 H_m^{(a)}}\right)$$

$$= 0.2 \text{ cm}\left(\frac{4}{2}\right)\left(\frac{1.0}{4\pi \times 10^{-7} \times 4 \times 10^4}\right)$$

$$= 7.96 \text{ cm}$$

(*b*) Figure 1-22*b* shows a series of load lines for the system with $A_g = 2 \text{ cm}^2$ and with current i applied to the excitation winding. The general equation for these load lines can be readily derived since from Eq. 1-5

$$Ni = H_m l_m + H_g g$$

and from Eqs. 1-3 and 1-7

$$B_m A_m = B_g A_g = \mu_0 H_g A_g$$

Thus

$$B_m = -\mu_0\left(\frac{A_g}{A_m}\right)\left(\frac{l_m}{g}\right)H_m + \frac{\mu_0 N}{g}\left(\frac{A_g}{A_m}\right)i$$

$$= \mu_0\left[-\left(\frac{2}{4}\right)\left(\frac{7.96}{0.2}\right)H_m + \frac{100}{2 \times 10^{-3}}\left(\frac{2}{4}\right)i\right]$$

$$= -2.50 \times 10^{-5} H_m + 3.14 \times 10^{-2} i$$

From Fig. 1-22*b* we see that if the plunger is set so that $A_g = 2\ \text{cm}^2$, the current in the magnetizing winding is increased to the value $i_{\max}$ where

$$i_{\max} = \frac{B_{\max} + 2.50 \times 10^{-5} H_{\max}}{3.14 \times 10^{-2}} \quad \text{A}$$

In this case, we do not have a complete hysteresis loop for Alnico 5, and hence we will have to estimate $B_{\max}$ and $H_{\max}$. Linearly extrapolating the B-H curve at $H = 0$ back to 4 times the coercivity, that is, $H_{\max} = 4 \times 50 = 200$ kA/m, yields $B_{\max} = 2.1$ T. This value is undoubtedly extreme and will overestimate the required current somewhat. However, using $B_{\max} = 2.1$ T and $H_{\max} = 200$ kA/m yields $i_{\max} = 22.6$ A.

Thus with the air-gap area set to 2 cm^2, increasing the current to 22.6 A and then reducing it to zero will achieve the desired magnetization.

(*c*) Because we do not have specific information about the slope of the recoil line, we assume that its slope is the same as that of the B-H characteristic at the point $H = 0$, $B = B_r$. From Fig. 1-22*a*, with the recoil line drawn with this slope, we see that as the air-gap area varies between 2 and 4 cm^2, the magnet flux density B_m varies between 1.00 and 1.08 T. Since the air-gap flux density equals A_m/A_g times this value, the air-gap flux density will equal $4/2(1.00) = 2.0$ T when $A_g = 2.0\ \text{cm}^2$ and $(4/4)(1.08) = 1.08$ T when $A_g = 4.0\ \text{cm}^2$.

As has been seen, hard magnetic materials such as Alnico 5 can be subject to demagnetization, should their operating point be varied excessively. As shown in Example 1-9, these materials can be stabilized with some loss in effective remanent magnetization. However, this procedure does not guarantee absolute stability of operation. For example, if the material in Example 1-9 were subjected to an air-gap area smaller than 2 cm^2 or to excessive demagnetizing current, the effect of the stabilization would be erased and the material would be found to operate on a new recoil line with further reduced magnetization.

However, many materials, such as samarium cobalt, ceramic 7, and neodymium-iron-boron (see Fig. 1-18), which have large values of coercivity, tend to have very low values of recoil permeability, and the recoil line is essentially tangent to the B-H characteristic for a large portion of the useful operating region. This can be seen in Fig. 1-18, which shows the dc magnetization curve for neodymium-iron-boron, from which we see that this material has a remanent magnetization of 1.25 T and a coercivity of −940 kA/m. The portion of the curve between these points is a straight line with a slope equal to $1.06\mu_0$, which is the same as the slope of its recoil line. As long as these materials are operated on this low incremental permeability portion of their B-H characteristic, they do not require stabilization, provided they are not excessively demagnetized.

t $A_g = 2$ cm^2, the
alue i_{max} where

loop for Alnico 5,
ırly extrapolating
ıat is, $H_{max} = 4 \times$
›ubtedly extreme
However, using

ıg the current to
›d magnetization.
t the slope of the
f the B-H charac-
th the recoil line
varies between 2
1.00 and 1.08 T.
value, the air-
$A_g = 2.0$ cm^2 and

Alnico 5 can be
be varied exces-
e stabilized with
r, this procedure
ımple, if the ma-
ıaller than 2 cm^2
ıbilization would
a new recoil line

, ceramic 7, and
ues of coercivity,
the recoil line is
ırtion of the use-
ch shows the dc
ıich we see that
d a coercivity of
ıts is a straight
slope of its recoil
ncremental per-
equire stabiliza-

1-7 SUMMARY

Electromechanical devices which employ magnetic fields often use ferromagnetic materials for guiding and concentrating these fields. Because the magnetic permeability of ferromagnetic materials can be large (up to tens of thousands times that of the surrounding space), most of the magnetic flux is confined to fairly definite paths determined by the magnetic material. In addition, often the frequencies of interest are low enough to permit the magnetic fields to be considered quasi-static, and hence they can be determined simply from a knowledge of the net mmf acting on the magnetic structure.

As a result, the solution for the magnetic fields in these devices can be obtained in a straightforward fashion by using the techniques of magnetic circuit analysis. These techniques can be used to reduce a complex three-dimensional magnetic field solution to what is essentially a one-dimensional problem. As in all engineering solutions, a certain amount of experience and judgment is required, but the technique gives useful results in many situations of practical engineering interest.

Ferromagnetic materials are available with a wide variety of characteristics. In general, their behavior is nonlinear, and their B-H characteristics are often represented in the form of a family of hysteresis (B-H) loops. Losses, both hysteretic and eddy-current, are a function of the flux level and frequency of operation as well as the material composition and the manufacturing process used. A basic understanding of the nature of these phenomena is extremely useful in the application of these materials in practical devices. Typically, important properties are available in the form of curves supplied by the material manufacturers.

Certain magnetic materials, commonly known as hard or permanent magnet materials, are characterized by large values of remanent magnetization and coercivity. These materials produce significant magnetic flux even in magnetic circuits with air gaps. With proper design they can be made to operate stably in situations which subject them to a wide range of destabilizing forces and mmf's. Permanent magnets find application in many small devices, including loudspeakers, ac and dc motors, microphones, and analog electric meters.

PROBLEMS

1-1. A magnetic circuit with a single air gap is shown in Fig. 1-23. The core dimensions are

Cross-sectional area $A_c = 1.5 \times 10^{-3}$ m^2
Mean core length $l_c = 0.7$ m
Gap length $g = 2.5 \times 10^{-3}$ m
$N = 75$ turns